

1 An unbiased comparison of immunoglobulin sequence 2 aligners

3 Thomas Konstantinovsky^{1,2,*}, Ayelet Peres^{1,2,*}, Pazit Polak^{1,2} and Gur Yaari^{1,2,3,†}

4 ¹Faculty of Engineering, Bar Ilan University, 5290002 Ramat Gan, Israel

5 ²Bar Ilan institute of nanotechnology and advanced materials, Bar Ilan university, 5290002
6 Ramat Gan, Israel

7 ³Department of Pathology, Yale School of Medicine, New Haven, CT, USA

8 *These authors contributed equally to this work.

9 [†]To whom correspondence should be addressed. Email: gur.yaari@biu.ac.il

10 June 11, 2024

11 **Abstract**

12 Adaptive Immune Receptor Repertoire sequencing (AIRR-seq) is critical for our under-
13 standing of the adaptive immune system's dynamics in health and disease. Reliable analysis
14 of AIRR-seq data depends on accurate Immunoglobulin (Ig) sequence alignment. Various Ig
15 sequence aligners exist, but there is no unified benchmarking standard representing the com-
16 plexities of AIRR-seq data, obscuring objective comparisons of aligners across tasks. Here, we
17 introduce GenAIRR, an efficient simulation framework for generating Ig sequences alongside
18 their ground truths. GenAIRR realistically simulates the intricacies of V(D)J recombination,
19 somatic hypermutation, and an array of sequence corruptions. We comprehensively assessed
20 prominent Ig sequence aligners across various metrics, unveiling unique performance char-
21 acteristics for each aligner. The GenAIRR-produced datasets, combined with the proposed
22 rigorous evaluation criteria, establish a solid basis for unbiased benchmarking of immuno-
23 genetics computational tools. It sets up the ground for further improving the crucial task of
24 Ig sequence alignment, ultimately enhancing our understanding of adaptive immunity.

25 **1 Introduction**

26 The adaptive immune system functionality relies upon a diverse and dynamic set of cell recep-
27 tors. In lymphocytes, this diversity originates from the V(D)J recombination process [26], with B
28 cells undergoing further diversification through affinity maturation; a process that includes clonal
29 expansion [17], somatic hypermutation (SHM) [27], and affinity-dependent selection [45]. Ad-
30 vances in sequencing technologies, particularly adaptive immune receptor repertoire sequencing

31 (AIRR-seq)[22], have profoundly enhanced our understanding of this repertoire, providing detailed insights into its dynamics and diversity in response to a wide spectrum of immunological challenges [42, 41, 19, 9, 2, 15, 37].

32 Analyzing AIRR-seq data requires an accurate alignment of immunoglobulin (Ig) sequences to their germline ancestors. This task poses significant computational challenges due to factors such as the vast array of known germline sequences [5], the stochastic nature of gene trimming during V(D)J recombination [39], alterations introduced by SHM [46], and ambiguities resulting from sequencing errors [44].

33 To address these challenges, two primary approaches are utilized for aligning Ig sequences: string distance metrics-based and Hidden Markov Models (HMM)-based. Distance-based methods [4, 48, 3], while computationally efficient, may encounter difficulties with complex sequence variations such as insertions, deletions, and mutations. In contrast, HMM-based methods [12, 25, 35] leverage probabilistic models to capture some of the stochastic nature of V(D)J recombination and sequence evolution. This approach provides a more detailed representation of the real diversity of Ig sequences and somatic evolutionary patterns. However, these methods can require more computational resources and rely on parameters inferred from empirical, potentially noisy, datasets.

34 All tools for Ig sequence alignment require a germline reference set that encompasses the known alleles expected to be included in AIRR-seq data. This germline reference set is used to establish the metrics necessary for the alignment. Current germline reference sets, such as those from IMGT [21] and OGRDB [20], suffer from either noise or incompleteness, further complicating alignment tasks. Thus, an adaptable germline reference set is essential for several reasons. First, numerous more recent studies have identified novel Ig alleles that are not present in standard reference databases (e.g., [14, 23, 36, 24, 13, 28]). These newly identified alleles significantly contribute to immune repertoire diversity and play a crucial role in accurate alignment and analysis in personalized genomics [11, 10, 7, 35]. The importance of personalized genomics cannot be overstated, as individuals may have unique variations in their Ig genes, affecting immune responses and disease susceptibilities [6, 30, 8, 34, 47, 1, 18]. Furthermore, the ability to modify the reference to accommodate personalized genotypes ensures precise alignment and interpretation of Ig sequences. This adaptability also assists in identifying rare and low-frequency variants that may be critical to immune function but are often disregarded in standard reference-based alignments during immune repertoire analysis [32].

35 Understanding whether an Ig sequence is productive, or expressed, is vital for various aspects of immunological research. Since many factors contribute to the ability to express an Ig, only experimental validation can confirm the productivity status of a sequence. Nevertheless, several necessary conditions must be met for a sequence to be considered productive, which were identified originally by the International ImMunoGeneTics Information System (IMGT). The standardized framework to computationally infer the productivity of Ig sequences [33] includes ensuring a correct open reading frame; the absence of aberrations in the start codon, splicing sites, and regulatory elements; the absence of internal stop codons; and an in-frame junction region where the V, D, and J gene segments align properly. Despite these standardized criteria, variations in the assessment of sequence productivity can arise due to differences in algorithms and methodologies used by the different sequence aligners. Factors such as the handling of ambiguous gene segment boundaries,

74 treatment of sequencing errors, and interpretation of junction regions can lead to discrepancies in
75 sequence productivity classifications among aligners.

76 To address these challenges and accurately evaluate alignment tools, past benchmarks often
77 used datasets derived from or simulated based on direct sequencing efforts [48, 40, 35]. These
78 datasets inherently carry biases, like unequal allele representation and batch-effects prevalent in
79 many cohorts. In addition, these benchmarks often overlooked critical aspects such as the ability
80 of aligners to handle insertion or deletions (indels), accurately define the start and end positions of
81 segments, and stratify performance across different levels of SHM. Further, the IGH/IGK/IGL ge-
82 nomic loci display high variability among individuals, posing challenges in creating representative
83 reference sets. Such challenges underscore the need for a more comprehensive and unbiased bench-
84 marking approach. The benefits of using objectively simulated data in such tasks is of paramount
85 importance [38].

86 Building upon these insights, we propose a two-fold approach to address the challenges in
87 benchmarking alignment tools effectively. First, we present a benchmarking setup that encom-
88 passes three critical metrics for evaluating sequence alignment tools: 1) Assessment of the tools'
89 accuracy in correctly identifying sequence allele calls. This precision is fundamental, as it forms
90 the basis for understanding the alleles and genes at play, with significant downstream impacts
91 on analyses such as genotype determination [29, 7], haplotype inference [31], cloning [44, 16],
92 and SHM calls. 2) Segmentation: aiming to precisely identify the start and end of alleles within
93 the sequence. Precision in this task is crucial because incorrect segmentation, such as prema-
94 ture or late trimming of the 3' end of the V allele can lead to missed SHM events, influence the
95 productivity assessment, or erroneous identification of non-real SHM events. 3) Productivity as-
96 sessment of sequences. Downstream analysis pipelines commonly filter out what they consider
97 to be non-productive sequences, hence correct assessment by the aligners has a high impact. Al-
98 though evaluating productivity may seem straightforward, differences between aligners arise from
99 variations in their algorithms and implementations. Second, we introduce GenAIRR, a robust
100 simulation framework designed to generate Ig sequence datasets with established ground truths
101 that enable accurate and comprehensive comparisons among aligners. GenAIRR incorporates re-
102 alistic sequence corruptions and noise, filling gaps in existing simulation frameworks and providing
103 a solid foundation for a robust benchmarking setup. See Supplementary Table 1 for an overview
104 of existing simulation frameworks.

105 This manuscript aims not only to elevate the standards of aligner comparison, but also to estab-
106 lish a comprehensive framework for the ongoing evaluation of both existing and newly developed
107 alignment methodologies. By doing so, it seeks to significantly improve the precision and reliability
108 of AIRR-seq analysis. Such advancements will deepen our understanding of the adaptive immune
109 system's responses to pathogens and enhance our ability to leverage this knowledge in health and
110 disease contexts.

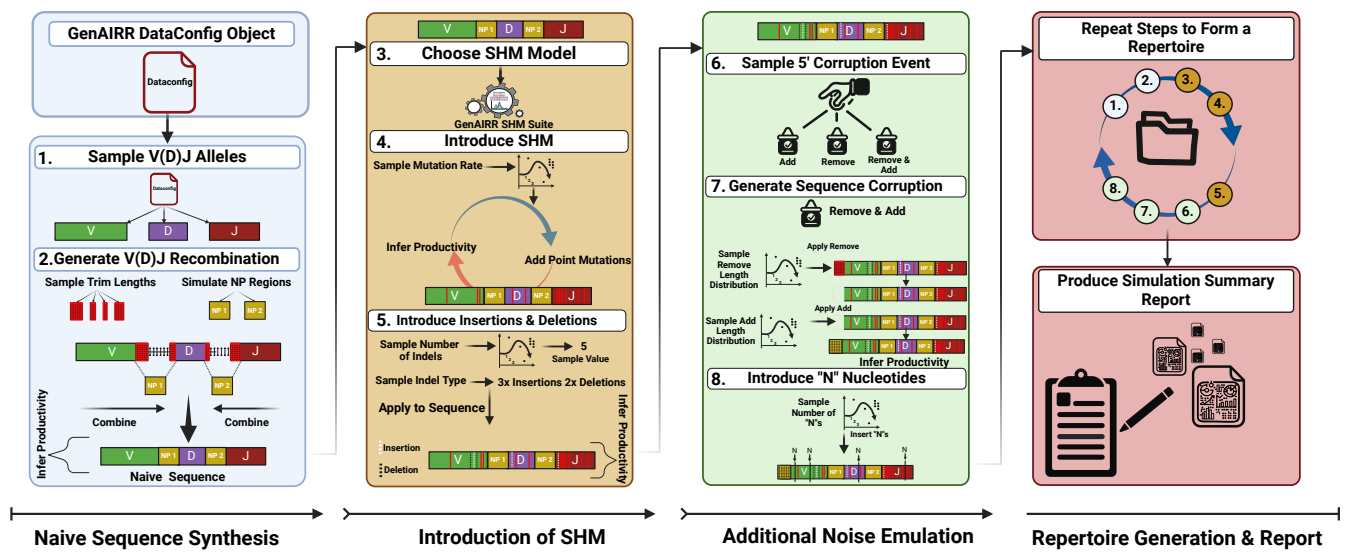


Figure 1: **GenAIRR modular architecture to simulate Ig sequences.** The first column (steps 1-2) describes simulation of a naive Ig sequence using the provided configuration file (Data-Config). The second column (steps 3-5) illustrates the introduction of alterations to the simulated sequence, such as SHM and indels. The third column (steps 6-7) illustrates the introduction of further experimental noise to the simulated sequence, including 5' corruptions and N nucleotides. Finally, the fourth column illustrates that GenAIRR allows for repeating the sequence simulation to form a repertoire and generating a report summarizing its statistical properties.

111 2 Results

112 2.1 Creating a benchmarking setup using GenAIRR

113 To establish a robust benchmarking setup, a bias-free dataset is required. For this, we created
 114 GenAIRR, an AIRR-seq data simulator that simulates the full spectrum of V(D)J recombination
 115 events and introduces realistic sequence corruptions such as 5' nucleotide trimming or addition,
 116 masking nucleotides with Ns, and introduction of indels. GenAIRR mitigates biases by enabling
 117 simulations without relying on empirical data distribution, opting instead for a uniform distribution
 118 to generate sequences (refer to Supplementary Table 1 for comparisons with other simulation
 119 tools). In addition, GenAIRR's modular architecture allows users to tailor simulations to reflect
 120 specific experimental conditions. GenAIRR provides comprehensive ground truth data for each
 121 simulated sequence, including allele calls, segmentation positions, and productivity assessments,
 122 formatted in the AIRR community schema for annotated AIRR-seq data [43]. This facilitates
 123 straightforward comparisons with the output of commonly used alignment tools. GenAIRR is
 124 illustrated in Figure 1.

125 Using GenAIRR, we created three datasets, each containing 6 million sequences, with a uniform
 126 distribution of alleles. The first dataset (DS1) consisted solely of productive sequences, devoid of

127 corruptions, N masks, or indels, but did include varying mutation rates to mimic real AIRR-seq
128 data. The second dataset (DS2) included mainly nonproductive sequences, resulting from the
129 rearrangement process, introduction of mutations, or corruption events such as 5' trimming or
130 addition, N insertions, and indels (refer to Supplementary Table 3 for simulation details).

131 We used the GenAIRR report feature to check how alleles are distributed in these datasets.
132 Although we aimed for an even distribution, we noticed a small difference in the usage of certain
133 V and J alleles in DS1 (Fig. 2A and C) compared to DS2 (Supplementary Fig. 3A and C). This
134 difference stems from constraints inherent in the generation process of productive sequences.

135 In simulating D alleles, the protocol involved trimming both the 5' and 3' ends, sometimes
136 resulting in very short sequences that pose alignment challenges due to their potential to match
137 multiple alleles (see method section 4.2). In actual AIRR-seq data, it is impossible to ascertain the
138 origin of these short D sequences. Hence, GenAIRR incorporates a feature that identifies sequences
139 of five or fewer nucleotides as "Short-D" and conceals their origin. In both DS1 (Fig. 2B) and
140 DS2 (Supplementary Fig. 3B), the allele usage across other D alleles was generally uniform. The
141 simulated datasets exhibited a distribution of CDR3 lengths that resembled empirical data (Fig.
142 2D, Supplementary Fig. 3D).

143 2.2 Benchmarking immunoglobulin sequence aligners

144 In the presented benchmark evaluation, we first surveyed the existing alignment tools, and selected
145 four widely used aligners, IgBLAST [48], MiXCR [3], HighV-QUEST [4], and Partis [35], based
146 on their popularity, compatibility with the AIRR community schema for annotated AIRR-seq
147 data [43], consistent support, and active development within the immunogenetics community (see
148 Supplementary Table 2 for a summary). Importantly, these aligners were also chosen for their
149 diverse alignment methodologies. IgBLAST employs BLAST for alignment, HighV-QUEST and
150 MiXCR utilize multiple sequence alignment techniques, and Partis adopts an HMM approach.

151 Here, we utilized the newly published reference set by the AIRR community [5], which requires
152 the aligners to enable the use of a custom reference set. HighV-QUEST is the only aligner of the
153 four that is unable to accept a custom reference set, and thus in cases where the resulting allele
154 assignment HighV-QUEST produced was not included in the AIRR-C reference set, we matched it
155 with the closest allele in the set. Not all aligners return results for every sequence in the datasets.
156 In DS1, IgBLAST, Partis, and HighV-QUEST provided assignments for all 6 million sequences at
157 the V allele level, while MiXCR had a retrieval rate of approximately 89% (Fig. 2E). Furthermore,
158 Partis consistently had a retrieval rate of 100% for both the D and the J alleles, closely followed by
159 HighV-QUEST with ~99%. The retrieval rate of IgBLAST for J alleles is roughly 99% and 96%
160 for the D alleles. MiXCR showed a lower retrieval rate at 89% for J alleles and 87% for D alleles
161 (Fig. 2F-G). The trend remained the same for the nonproductive sequences, with Partis returning
162 the highest retrieval rate, trailed by IgBLAST, then IMGT, and lastly MiXCR (Supplementary
163 Fig. 3E-G).

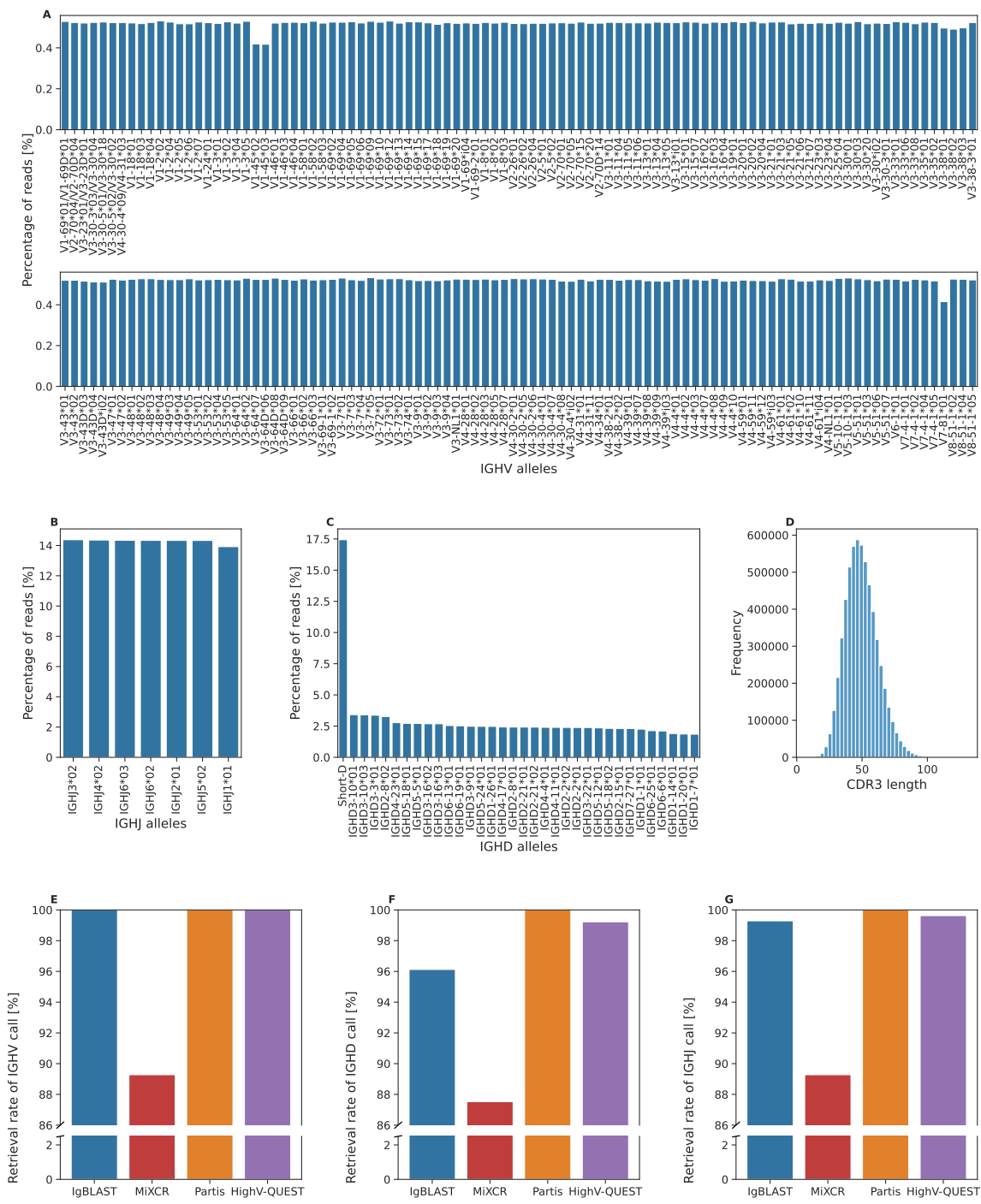


Figure 2: Overview of the simulated productive dataset. (A-C) Distribution of the V, D, and J allele usage in the productive dataset. Each column represents a different allele, and the y-axis indicates their relative usage percentage in the dataset. (D) CDR3 length distribution. The x-axis shows the CDR3 lengths, and the y-axis indicates their frequency. (E-G) Aligners allele assignment retrieval rate. Each column represents a different aligner, and the y-axis shows the percentage of sequences for which the aligner returned an allele assignment. The colors correspond to the different aligners: blue for IgBLAST, red for MiXCR, orange for Partis, and purple for HighV-QUEST.

164 2.3 Precision of Aligners Varies with Segment Mutation Rates and 165 Lengths

166 We evaluated the aligners' ability to accurately assign V, D, and J allele calls for each sequence.
167 We observed variations in performance across different mutation rates and sequence lengths (Fig.
168 3). IgBLAST demonstrated the highest overall accuracy in assigning V alleles. However, MiXCR
169 excelled in sequences with a mutation rate of up to 10%, but rapidly declined at higher rates. No-
170 tably, HighV-QUEST exhibited underperformance at lower mutation rates but showed a relatively
171 steady, good accuracy in highly mutated sequences (Fig. 3A).

172 Assigning the J allele was a relatively easier task due to the reduced variability among alleles.
173 Partis consistently outperformed all aligners across various mutation rates, with IgBLAST closely
174 following but showing a decline in sequences with over a 17% mutation rate. MiXCR maintained
175 good accuracy up to a mutation rate of 11%, but, as with V alleles, its performance declined at
176 higher mutation rates compared to other aligners (Fig. 3 B).

177 The evaluation of D assignment performance is shown as a function of D segment length rather
178 than mutation rate. This is because mutation rates can vary significantly due to the short segment
179 lengths, potentially masking the influence of both factors (Fig. 3C). For longer D sequences, Partis
180 and IgBLAST exhibited slightly superior performance, with MiXCR lagging behind. For shorter
181 D segments, IgBLAST remained the top performer, while HighV-QUEST exhibited the lowest
182 agreement with ground truth. These findings underscore the nuanced performance dynamics of
183 aligners depending on mutation rates and sequence lengths. To further assess the impact of segment
184 length on accuracy, we isolated sequences that did not encounter any mutations within the IGHD
185 segment (Fig. 3D). The accuracy of all aligners spiked across all segment lengths, with IgBLAST
186 demonstrating accuracy above 90% for sequences longer than 9 nucleotides. However, as observed
187 in Fig. 3C, accuracy declines in short D segments, emphasizing the influence of segment length on
188 the ability to correctly assign the D allele.

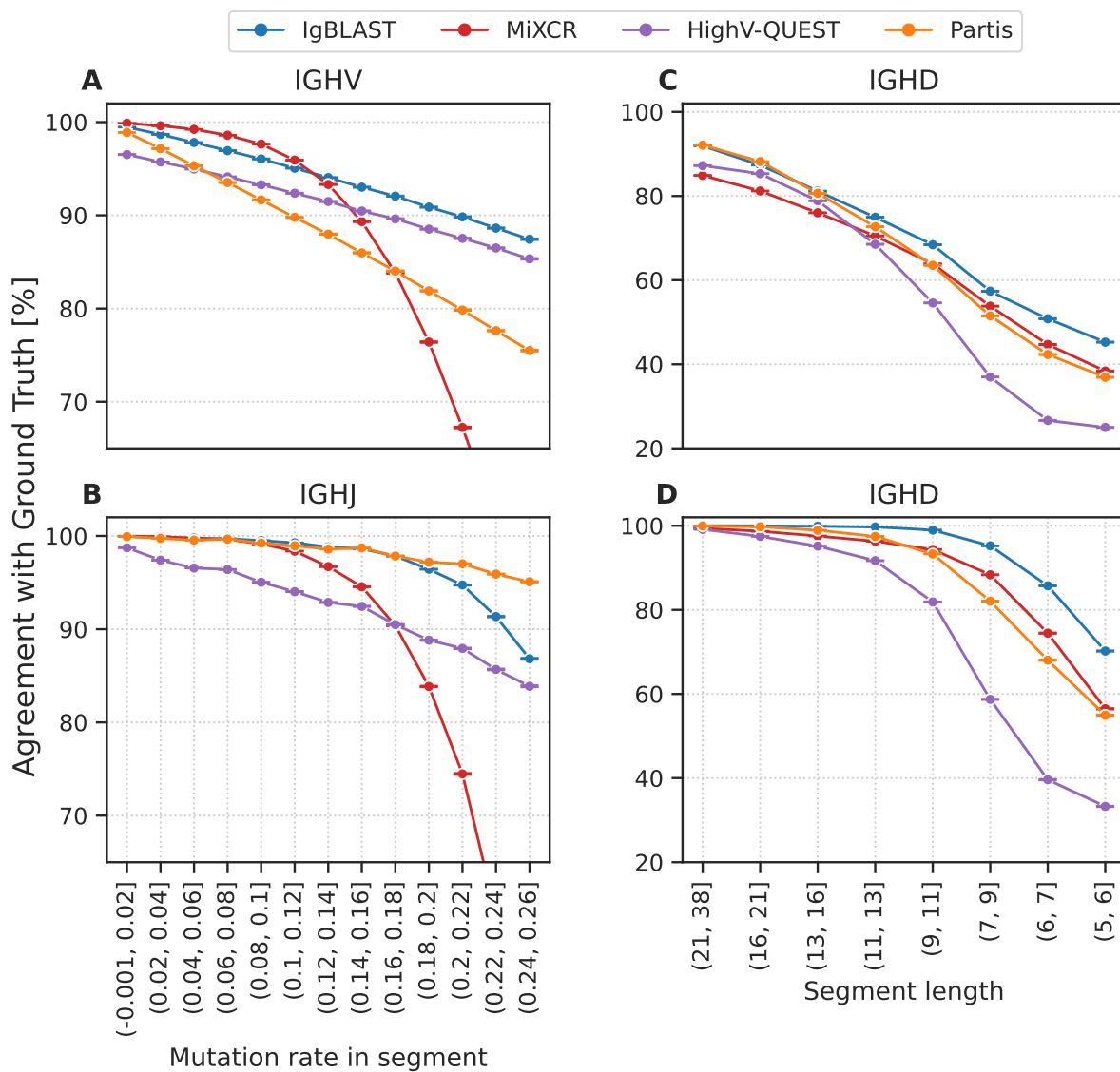


Figure 3: **Aligners predictive performance of allele calls.** (A+B) Agreement with ground truth for IGHV (A) and IGHJ (B) segment calls across varying mutation rates. The x-axis represents the mutation rates ranging from 0.01 to 0.25, and the y-axis shows the agreement percentage with the true allele call. The colors correspond to the aligners as indicated in the figure. (C) Agreement with ground truth for IGHD segment calls across varying segment lengths. The x-axis represents the varying D segment lengths from 38 to 6, and the y-axis shows the agreement percentage with the true allele call. (D) Same as C) for sequences with 0 mutations in their D segments.

189 2.4 Segmentation position accuracy differs among aligners

190 Besides accurately identifying alleles in AIRR-seq alignment, another crucial task is segmenting
191 the sequence into distinct allele regions, which facilitates the correct attribution of SHM events.
192 To evaluate the accuracy of segmentation by the aligners, we utilized both DS1 and DS2. We
193 computed the Root Mean Square Error (RMSE) for each segment's 5' and 3' positions across all
194 aligners. To minimize bias, we only considered perfect matches between allele calls and the ground
195 truth, prioritizing the first matching call in cases of multiple allele calls and excluding V 5' and J
196 3' segmentations for this analysis.

197 In DS1, the RMSE results for the V 3' position were generally similar across the aligners,
198 except MiXCR, which exhibited a higher value (Fig. 4A). The accuracy in segmenting the D
199 5' position was consistent across all aligners. However, for the D 3' position, Partis showed a
200 slightly higher RMSE value compared to the others. Regarding the J 5' position, HighV-QUEST
201 recorded the highest RMSE, while Partis demonstrated the lowest value. In DS2, the aligners
202 maintained relatively similar RMSE and ranking values, as observed in DS1 (Fig. 4B). These
203 findings underscore the significant disparities in segmentation accuracy across aligners and their
204 performance across different dataset contexts.

205 2.5 Aligners Accuracy in Determining Sequence Productivity

206 Sequence productivity is important for immune repertoire analysis tools, affecting their precision
207 in tasks such as genotype, haplotype, clonality, and diversity assessments. To assess the accuracy
208 of the aligners in evaluating sequence productivity, we initially established the ground truth using
209 GenAIRR. GenAIRR determines sequence productivity based on the following criteria: absence of
210 a stop codon, presence of conserved AA at the start and end of the junction, and alignment that
211 is in-frame (Supplementary Figure 2). To assess aligner accuracy in determining productivity, we
212 used dataset DS3, which contains four million randomly sampled productive sequence from DS1,
213 and a matching number of randomly sampled nonproductive sequence from DS2.

214 For productive sequences, Partis demonstrated perfect accuracy, whereas IgBLAST showed a
215 low error rate with a slightly higher rate of missing sequences, marginally outperforming HighV-
216 QUEST, which had a higher error rate but no missing sequences. Lastly, MiXCR exhibited a
217 higher error rate and the most substantial rate of missing sequences (Fig. 4C, left column). The
218 pattern was comparable for nonproductive sequences. Partis showed the highest accuracy, with a
219 small proportion of sequences missing. IgBLAST performed slightly better than HighV-QUEST
220 in terms of error rates. MiXCR exhibited a high error rate and the largest proportion of missing
221 sequences (Fig. 4C right column).

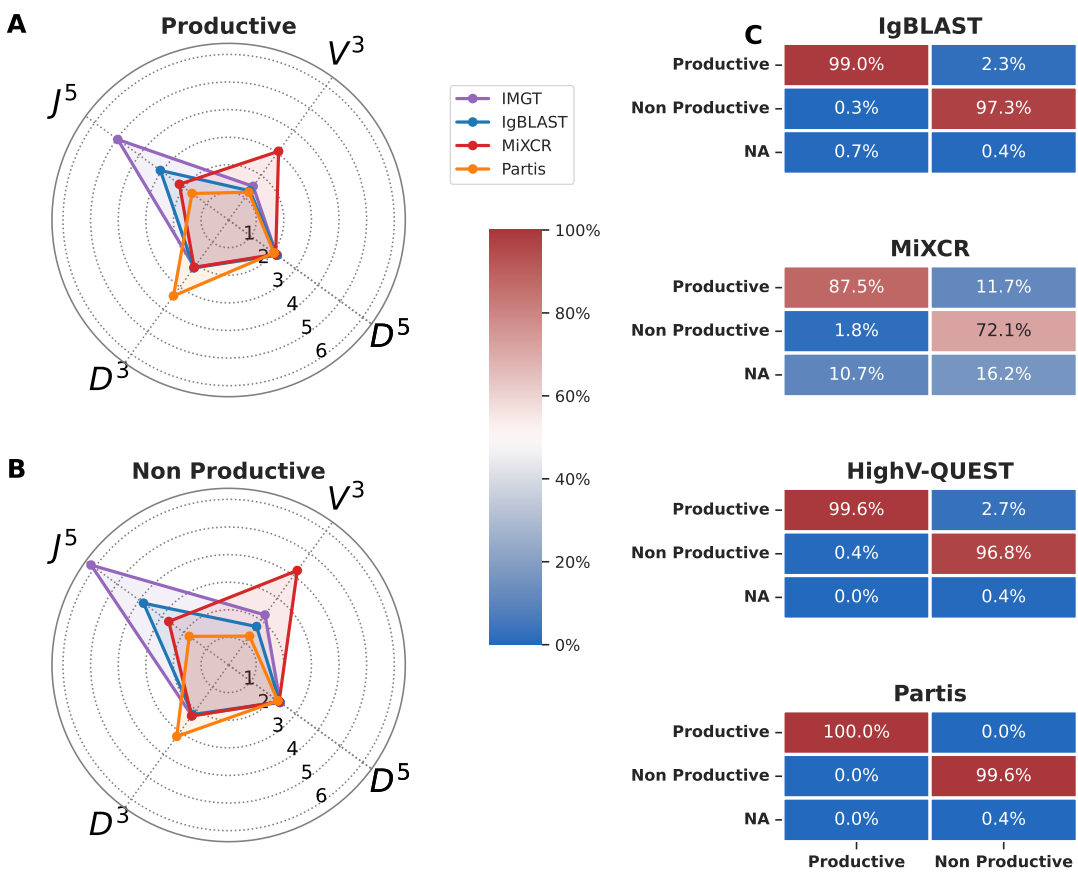


Figure 4: **Aligners segmentation and productivity assessment.** (A+B) Radar charts illustration of the RMSE (Root Mean Square Error) values for segmentation accuracy across gene segment start and end positions (V3, D3, D5, J3) in productive (A) and non-productive (B) sequences. (C) The confusion matrices provide an accuracy comparison of productive assessments. In each matrix, columns represent the 4M sequence subset of the simulated dataset, while rows represent the aligners' productive assessment categorized as Productive, Non Productive, or NA (indicating no assessment for the sequence). The value in each cell indicates the percentage of agreement with the ground truth. The color scale reflects the level of accuracy.

222 3 Discussion

223 The current study represents an unbiased evaluation of Ig sequence aligners, facilitated by the
 224 GenAIRR simulation framework. This comprehensive assessment across multiple metrics has out-
 225 lined distinct strengths and weaknesses inherent in the widely used aligners IgBLAST, MiXCR,
 226 HighV-QUEST, and Partis. The datasets generated by GenAIRR provide a robust, unbiased
 227 platform for benchmarking these aligners in a spectrum of challenging immunogenetic variables,
 228 mimicking real-world complexities. This benchmarking analysis explores how noise levels, such as
 229 mutation rates and corruption events, affect aligner agreement with the ground truth. The align-
 230 ers' comparisons (Table 1) revealed varying performances. MiXCR emerged as the most efficient

aligner in terms of runtime and was the top performer for V assignment accuracy at low mutation rates (<10%), but decreased dramatically at higher mutation rates. Moreover, it showed lower accuracy for D assignment across all segment lengths. IgBLAST, although >10 times slower than MiXCR, outperformed the other aligners in almost all allele assignment accuracies. One exception is Partis, which demonstrated excellent performance in J assignment accuracy across both low and high mutation rates. The accuracy metric used here for allele assignment is relatively lenient, requiring a single assignment per sequence to match the ground truth. This leniency can disadvantage aligners that, by default, return only one assignment, such as Partis, as they have a lower probability of matching the ground truth. Note that erroneous assignments can in many cases be rectified by inferring a personal genotype.

Properly segmenting a sequence can influence factors such as attributing SHM events to the correct segments and assessing sequence productivity. Partis showed the lowest RMSE for position predictions in most categories, and the highest accuracy in the productivity assessment. Error rates in productivity can be attributed not only to segmentation errors, which can lead to missed stop codons, but also to misclassifying sequences that lack conserved residues in the junction as productive.

Criteria	IgBLAST		MiXCR		HighV-QUEST		partis	
	Prod.	Non	Prod.	Non	Prod.	Non	Prod.	Non
Accepts Custom Reference	✓		✓		✗		✓	
6M Seqs Runtime (Minutes)	2200		200		—		5400	
V Accuracy (MR < 10%)	97.79	97.57	98.99	97.78	94.21	94.61	95.31	93.43
V Accuracy (MR > 10%)	90.78	89.99	75.09	66.92	88.45	88.18	81.77	80.79
J Accuracy (MR < 10%)	99.74	99.61	99.69	99.34	96.83	95.14	99.62	99.24
J Accuracy (MR > 10%)	93.69	92.49	70.86	68.85	88.48	86.58	97.0	96.86
D Accuracy (Length < 10)	51.14	49.42	45.63	42.44	29.53	26.73	43.57	42.47
D Accuracy (Length > 10)	85.3	84.16	79.26	74.75	80.36	75.52	84.69	83.81
V 3' RMSE	1.31	1.72	3.08	4.23	1.51	2.24	1.24	1.29
D 5' RMSE	2.17	2.29	2.11	2.26	2.15	2.31	2.03	2.2
D 3' RMSE	2.14	2.22	2.12	2.28	2.11	2.27	3.4	3.2
J 5' RMSE	3.06	3.81	2.2	2.68	4.96	6.16	1.64	1.76
Productivity Accuracy	99	97.3	87.5	72.1	99.6	96.8	100	99.6

Table 1: Comparison of different IG sequence aligners focusing on criteria such as custom reference acceptance, operational efficiency, and accuracy across mutation rates (MR). Accuracy metrics are presented for productive (left) and non-productive (right) sequences, with the best results highlighted in **bold**. RMSE (Root Mean Square Error) quantifies the precision of segment start and end position predictions; lower values indicate higher precision.

GenAIRR's modularity is a standout feature, allowing the simulation to start from a naive sequence and progressively introduce noise (Table 2). This modular design facilitates easy adaptation of the code to different noise models and addition of optional stages, such as simulating epigenetic modifications, incorporating complex recombination patterns, or adding sophisticated

251 SHM models. GenAIRR is released as an open source code, to allow community contributions
252 to the simulation framework that may enhance its versatility and utility beyond the application
253 presented here. Here, we used GenAIRR to simulate human Ig sequences, but other species can
254 present different challenges. For example, macaque monkeys have many more known V(D)J alle-
255 les [49] compared to human, and as such can affect aligner performances in a non-trivial manner.

256 In conclusion, our study not only presents a robust benchmarking setup for refining existing
257 alignment tools and encouraging the development of new ones, but also underscores the immense
258 potential of GenAIRR's modular and adaptable framework. By integrating advanced functionali-
259 ties and addressing key challenges in simulating Ig sequences, we pave the way for more accurate
260 and reliable bioinformatics tools in immunogenetics. This collaborative effort, coupled with stan-
261 dardized benchmarking criteria using simulated sequences with known ground truth, propels the
262 field towards optimized algorithms and deeper insights into immune system analysis, ultimately
263 benefiting healthcare and disease research.

264 4 Methods (online)

265 4.1 Simulation Workflow of GenAIRR

266 The GenAIRR simulation framework consists of a series of customizable modular events designed
267 to generate Ig sequences that reflect the complexity and variability found in natural immune
268 responses. Each event is controlled by a set of adjustable parameters, providing a high degree of
269 flexibility and coverage.

270 The simulation begins with a stochastic selection of variable (V), diversity (D), and joining
271 (J) alleles from a representative pool. In the context of the current manuscript, the aim was to
272 generate datasets with a uniform representation of all alleles. Once selected, the allele sequences
273 undergo specific trimming processes to enhance their structural complexity. Additionally, the
274 nontemplated, palindromic (NP) regions are integrated using Markov chains derived from empir-
275 ical data, which model the probabilistic arrangement of nucleotides (see Supplementary Section
276 1). Next, the simulation incorporates controlled mutation rates, models of SHM, and indels to
277 enrich sequence diversity. GenAIRR also provides the option to introduce ambiguous 'N' bases
278 deliberately, to test the robustness of sequence alignment algorithms. Additionally, sequencing
279 artifacts are simulated, particularly at the 5' ends of V alleles to mimic shorter sequences and
280 5' untranslated region residuals. These features are introduced through tunable parameters that
281 control the type, probability, and extent of errors. A detailed overview of the simulation steps is
282 provided in Table 2, and an example of the tunable parameters used in this manuscript is provided
283 in Supplementary Table 3.

Step	Process	Optional	Productivity Test
1-2	Generate Naive Sequence	✗	✓
1-2	Adjust Segment Positions Post-Recombination	✗	✗
1-2	Include Indistinguishable V, J alleles from trimming	✗	✗
1-2	Include Indistinguishable D alleles from 5' and 3' trimming	✗	✗
1-2	Flag Sequence with Short D Alleles	✗	✗
3-4	Simulate SHM	✓	✓
5	Introduce Insertions/Deletions	✓	✓
6-7	Apply Corruption to 5' End of V Allele	✓	✓
8	Introduce Ambiguous 'N' Bases	✓	✗
8	Calculate Finalized Sequence Mutation Rate	✗	✗

Table 2: Illustration of the main GenAIRR sequence simulation workflow. Each numbered step corresponds to a stage in Figure 1. Steps marked as 'Optional' can be adjusted or omitted based on specific simulation needs, and steps marked under 'Productivity Test' indicate whether a productivity assessment is performed at this step.

284 4.2 Ground Truths Produced by GenAIRR

285 GenAIRR generates detailed ground truth data for each Ig sequence, which is essential for evaluating
286 the accuracy of sequence alignment tools. These data include information on the V, D, and
287 J allele calls, and their respective segment start and end positions. In addition, the ground truth
288 includes documentation of the mutations, trimmings, indels, productivity, and corruption events
289 (see Supplementary Table 4 for ground truth example).

290 During the simulation of Ig sequences, GenAIRR incorporates several strategies to address
291 challenges such as the potential ambiguities arising from trimming or corruption at the allele ends.
292 One significant challenge is the short length of D alleles, caused by their substantial trimming at
293 both the 5' and 3' ends during recombination. This often results in sequences retaining only a
294 minimal number of bases, making it impossible to distinguish these short sequences from multiple
295 D alleles. GenAIRR manages this by employing a hyperparameter threshold to determine the
296 minimal length for a D allele to be considered distinguishable post-recombination. Alleles shorter
297 than this threshold are labeled as "Short-D". The chosen threshold of five bases reflects a balance
298 between computational efficiency and biological realism, covering approximately 85% of D alleles,
299 as seen in Supplementary Figure 1. A map object post-trimming identifies which alleles become
300 indistinguishable under specific scenarios, and adjustments to the ground truth are made. This
301 includes corrections to the start and end positions of each allele following recombination and the
302 simulated insertion of NP regions to verify that the trimmed section was not partially reconstructed
303 by the NP regions. Such careful adjustments maintain the integrity of the ground truth, enabling
304 more precise and reliable simulation outcomes (see Supplementary Section 2.1).

305 In addition to addressing these challenges, GenAIRR assesses the productivity of the simulated
306 sequence. The criteria for a productive sequence are the absence of stop codons, the sequence to
307 be in the correct open reading frame, and the presence of two conserved amino acids (AA) before

308 and after the Complementary Determining Region 3 (CDR3). The region encompassing these
309 conserved AAs and CDR3 is termed the junction. Sequence productivity is assessed four times
310 during the GenAIRR sequence simulation (refer to Table 2, and Supplementary Fig. 2).

311 4.3 Benchmarking setup

312 For creating our benchmarking setup, we have generated three datasets, created four comparison
313 matrices, and selected suitable alignment tools for comparison.

314 4.3.1 Data Preparation

315 Using GenAIRR, two datasets, each containing 6 million sequences, were simulated for this study.
316 These datasets were generated using the AIRR-C reference set [5] and clustered using the Allele
317 Similarity Cluster method [32] to remove identical sequences. Within this reference set, there are
318 192 V alleles, 33 D alleles, and 7 J alleles. The selection of alleles for the simulated sequences
319 followed a uniform distribution. This approach aimed to achieve an equal representation of all
320 alleles in the reference and to eliminate any potential biases.

321 The first dataset, DS1, comprised purely productive sequences, reflecting common AIRR-seq
322 data, enabling us to evaluate alignment tools under typical conditions. Supplementary Table 3
323 shows the parameters used to generate this dataset. The second dataset, DS2, primarily consisted
324 of non-productive sequences resulting from recombination, SHM events, or noise introduction
325 (Supplementary Table 3). This allowed us to test the alignment tools under extreme conditions
326 and assess their performance. The third dataset, DS3, was used to assess productivity calls in a
327 combination of data from DS1 and DS2. In summary:

- 328 • **DS1:** Includes only productive sequences without introduced corruptions, representing op-
329 timal alignment scenarios.
- 330 • **DS2:** Contains sequences with intentional corruptions like ambiguous base maskings ('N's),
331 5' corruption events (removal or addition of nucleotides), and indels. This dataset comprises
332 mostly non-productive sequences, with a minor fraction of productive sequences.
- 333 • **DS3:** A combined dataset comprising sampled sequences from both DS1 and DS2. Specif-
334 ically, four million productive sequences were randomly sampled from DS1, along with four
335 million non-productive sequences from DS2.

336 4.4 Benchmarking Immunoglobulin Sequence Alignment tools

337 In this study, we surveyed the existing alignment tools (Supplementary Table 2), and selected four
338 popular tools for comparison. These tools were selected not only because of their popularity, but
339 also because they are consistently maintained and developed in the immunogenetics community,
340 and also comply with the AIRR community schema for annotated AIRR-seq data [43]. The leading
341 aligners that were evaluated here are IgBLAST[48], MiXCR[3], HighV-QUEST[4] by IMGT, and
342 Partis[35].

343 **4.4.1 Benchmarking Criteria**

344 To benchmark the performance of the aligners, we have used four metrics:

- 345 • **Alignment Accuracy:** The effectiveness with which each aligner identified V, D, and J
346 alleles under varying conditions of mutation rates and sequence corruptions was evaluated.
347 Accuracy was quantified using an "Agreement" metric, defined for each sequence as 1 if the
348 intersection of ground truth alleles (G) and alleles predicted by the aligner (P) is not empty
349 $G \cap P \neq \emptyset$, and 0 otherwise. This metric directly measures the ability of an aligner to
350 correctly identify alleles used to generate the sequence.
- 351 • **Segmentation Accuracy:** We evaluated aligners' precision in segmenting gene regions,
352 focusing on the accuracy of segment start and end positions amidst mutations and sequence
353 corruptions. This assessment is restricted to sequences for which there was a perfect match
354 between the aligners' allele calls for V, D, and J and the ground truth. In cases where the
355 aligner made multiple assignments for any of V, D, or J alleles, the sequence was included in
356 the comparison only if the first assignment matched the ground truth. This approach was
357 adopted because aligners' segmentation values are associated with the first assignment; hence,
358 including sequences with erroneous values from subsequent assignments would skew the anal-
359 ysis. An adjustment was made for Partis due to intentional N-padding at the beginning of
360 sequences. The results were modified to align Partis' segmentation positions accurately with
361 the ground truth by subtracting the added N-padding. To quantify segmentation errors, we
362 utilized the Root Mean Square Error (RMSE) metric, defined as:

$$RMSE = \sqrt{\frac{1}{n} \sum_{i=1}^n (P_i - G_i)^2}$$

363 where n is the number of sequences, P_i is the predicted segment position by an aligner, and
364 G_i is the actual ground truth position.

- 365 • **Productive Sequence Detection Accuracy:** This evaluation involved the calculation of
366 the proportion of true positives and true negatives, which were then utilized to determine
367 the overall classification accuracy. The results are presented using confusion matrices.
- 368 • **Runtime Efficiency and Resource Utilization:** The time needed to process 6 million
369 sequences was measured for each aligner to compare computational efficiency. This evaluation
370 was conducted on our cluster with specifications including an Intel(R) Xeon(R) Gold 6130
371 CPU @ 2.10GHz, 64 CPU cores, and 376 GB of RAM. The aligners were run on a single
372 thread without parallelization, to align 60,000 sequences. The processing time for this subset
373 was then multiplied by 100 to estimate the runtime for 6 million sequences.

374 **References**

375 [1] Yuval Avnir, Aimee S Tallarico, Quan Zhu, Andrew S Bennett, Gene Connelly, Jared Sheehan,
376 Jianhua Sui, Amr Fahmy, Chiung-yu Huang, Greg Cadwell, et al. Molecular signatures of

377 hemagglutinin stem-directed heterosubtypic human neutralizing antibodies against influenza
378 a viruses. *PLoS pathogens*, 10(5):e1004103, 2014.

379 [2] RJM Bashford-Rogers, Laura Bergamaschi, EF McKinney, DC Pombal, Federica Mescia,
380 JC Lee, DC Thomas, SM Flint, P Kellam, DRW Jayne, et al. Analysis of the b cell receptor
381 repertoire in six immune-mediated diseases. *Nature*, 574(7776):122–126, 2019.

382 [3] Dmitriy A Bolotin, Stanislav Poslavsky, Igor Mitrophanov, Mikhail Shugay, Ilgar Z Mame-
383 dov, Ekaterina V Putintseva, and Dmitriy M Chudakov. Mixer: software for comprehensive
384 adaptive immunity profiling. *Nature Methods*, 12(5):380–381, April 2015.

385 [4] X. Brochet, M.-P. Lefranc, and V. Giudicelli. Imgt/v-quest: the highly customized and
386 integrated system for ig and tr standardized v-j and v-d-j sequence analysis. *Nucleic Acids
387 Research*, 36(Web Server):W503–W508, May 2008.

388 [5] Andrew M Collins, Mats Ohlin, Martin Corcoran, James M Heather, Duncan Ralph, Mansun
389 Law, Jesus Martínez-Barnetche, Jian Ye, Eve Richardson, William S Gibson, et al. Airr-c ig
390 reference sets: curated sets of immunoglobulin heavy and light chain germline genes. *Frontiers
391 in Immunology*, 14:1330153, 2024.

392 [6] Andrew M Collins, Gur Yaari, Adrian J Shepherd, William Lees, and Corey T Watson.
393 Germline immunoglobulin genes: disease susceptibility genes hidden in plain sight? *Current
394 Opinion in Systems Biology*, 24:100–108, 2020.

395 [7] Martin M Corcoran, Ganesh E Phad, Néstor Vázquez Bernat, Christiane Stahl-Hennig,
396 Noriyuki Sumida, Mats AA Persson, Marcel Martin, and Gunilla B Karlsson Hedestam.
397 Production of individualized v gene databases reveals high levels of immunoglobulin genetic
398 diversity. *Nature communications*, 7(1):13642, 2016.

399 [8] Allan C Decamp, Martin M Corcoran, William J Fulp, Jordan R Willis, Christopher A Cot-
400 trell, Daniel LV Bader, Oleksandr Kalyuzhniy, David J Leggat, Kristen W Cohen, Ollivier
401 Hyrien, et al. Human immunoglobulin gene allelic variation impacts germline-targeting vac-
402 cine priming. *npj Vaccines*, 9(1):58, 2024.

403 [9] Ali H Ellebedy, Katherine JL Jackson, Haydn T Kissick, Helder I Nakaya, Carl W Davis,
404 Krishna M Roskin, Anita K McElroy, Christine M Oshansky, Rivka Elbein, Shine Thomas,
405 et al. Defining antigen-specific plasmablast and memory b cell subsets in human blood after
406 viral infection or vaccination. *Nature immunology*, 17(10):1226–1234, 2016.

407 [10] Daniel Gadala-Maria, Moriah Gidoni, Susanna Marquez, Jason A. Vander Heiden, Justin T.
408 Kos, Corey T. Watson, Kevin C. O'Connor, Gur Yaari, and Steven H. Kleinstein. Identifi-
409 cation of subject-specific immunoglobulin alleles from expressed repertoire sequencing data.
410 *Frontiers in Immunology*, 10:129, 2019.

411 [11] Daniel Gadala-Maria, Gur Yaari, Mohamed Uduman, and Steven H. Kleinstein. Auto-
412 mated analysis of high-throughput b-cell sequencing data reveals a high frequency of novel

413 immunoglobulin v gene segment alleles. *Proceedings of the National Academy of Sciences*,
414 112(8):E862–E870, 2015.

415 [12] Bruno A. Gaëta, Harald R. Malming, Katherine J.L. Jackson, Michael E. Bain, Patrick Wil-
416 son, and Andrew M. Collins. ihmmune-align: hidden markov model-based alignment and
417 identification of germline genes in rearranged immunoglobulin gene sequences. *Bioinformat-
418 ics*, 23(13):1580–1587, April 2007.

419 [13] William S Gibson, Oscar L Rodriguez, Kaitlyn Shields, Catherine A Silver, Abdullah
420 Dorgham, Matthew Emery, Gintaras Deikus, Robert Sebra, Evan E Eichler, Ali Bashir, et al.
421 Characterization of the immunoglobulin lambda chain locus from diverse populations reveals
422 extensive genetic variation. *Genes & Immunity*, 24(1):21–31, 2023.

423 [14] Moriah Gidoni, Omri Snir, Ayelet Peres, Pazit Polak, Ida Lindeman, Ivana Mikocziova,
424 Vikas Kumar Sarna, Knut EA Lundin, Christopher Clouser, Francois Vigneault, et al. Mosaic
425 deletion patterns of the human antibody heavy chain gene locus shown by bayesian haplotyp-
426 ing. *Nature communications*, 10(1):1–14, 2019.

427 [15] Miri Gordin, Hagit Philip, Alona Zilberberg, Moriah Gidoni, Raanan Margalit, Christopher
428 Clouser, Kristofor Adams, Francois Vigneault, Irun R Cohen, Gur Yaari, et al. Breast cancer
429 is marked by specific, public t-cell receptor cdr3 regions shared by mice and humans. *PLoS
430 Computational Biology*, 17(1):e1008486, 2021.

431 [16] Namita T Gupta, Jason A Vander Heiden, Mohamed Uduman, Daniel Gadala-Maria, Gur
432 Yaari, and Steven H Kleinstein. Change-o: a toolkit for analyzing large-scale b cell im-
433 munoglobulin repertoire sequencing data. *Bioinformatics*, 31(20):3356–3358, 2015.

434 [17] Philip D Hodgkin, William R Heath, and Alan G Baxter. The clonal selection theory: 50
435 years since the revolution. *Nature immunology*, 8(10):1019–1026, 2007.

436 [18] Todd A Johnson, Yoichi Mashimo, Jer-Yuarn Wu, Dankyu Yoon, Akira Hata, Michiaki Kubo,
437 Atsushi Takahashi, Tatsuhiko Tsunoda, Kouichi Ozaki, Toshihiro Tanaka, et al. Association
438 of an ighv3-66 gene variant with kawasaki disease. *Journal of human genetics*, 66(5):475–489,
439 2021.

440 [19] Uri Laserson, Francois Vigneault, Daniel Gadala-Maria, Gur Yaari, Mohamed Uduman, Ja-
441 son A Vander Heiden, William Kelton, Sang Taek Jung, Yi Liu, Jonathan Laserson, et al.
442 High-resolution antibody dynamics of vaccine-induced immune responses. *Proceedings of the
443 National Academy of Sciences*, 111(13):4928–4933, 2014.

444 [20] William Lees, Christian E Busse, Martin Corcoran, Mats Ohlin, Cathrine Scheepers, Freder-
445 ick A Matsen IV, Gur Yaari, Corey T Watson, AIRR Community, Andrew Collins, et al.
446 Ogrdb: a reference database of inferred immune receptor genes. *Nucleic acids research*,
447 48(D1):D964–D970, 2020.

448 [21] Marie-Paule Lefranc, Veronique Giudicelli, Chantal Ginestoux, Joumana Jabado-Michaloud,
449 Geraldine Folch, Fatena Bellahcene, Yan Wu, Elodie Gemrot, Xavier Brochet, Jero^me Lane,
450 et al. Imgt(R), the international immunogenetics information system(R). *Nucleic acids research*,
451 37(suppl_1):D1006–D1012, 2009.

452 [22] Vanessa Mhanna, Habib Bashour, Khang Lê Quy, Pierre Barennes, Puneet Rawat, Victor
453 Greiff, and Encarnita Mariotti-Ferrandiz. Adaptive immune receptor repertoire analysis. *Nature
454 Reviews Methods Primers*, 4(1):6, 2024.

455 [23] Ivana Mikocziova, Moriah Gidoni, Ida Lindeman, Ayelet Peres, Omri Snir, Gur Yaari, and
456 Ludvig M Sollid. Polymorphisms in human immunoglobulin heavy chain variable genes and
457 their upstream regions. *Nucleic Acids Research*, 48(10):5499–5510, 2020.

458 [24] Ivana Mikocziova, Ayelet Peres, Moriah Gidoni, Victor Greiff, Gur Yaari, and Ludvig M Sollid.
459 Germline polymorphisms and alternative splicing of human immunoglobulin light chain genes.
460 *Iscience*, 24(10), 2021.

461 [25] Supriya Munshaw and Thomas B. Kepler. Soda2: a hidden markov model approach for
462 identification of immunoglobulin rearrangements. *Bioinformatics*, 26(7):867–872, February
463 2010.

464 [26] Kenneth Murphy and Casey Weaver. *Janeway's immunobiology*. Garland science, 2016.

465 [27] Valerie H Odegard and David G Schatz. Targeting of somatic hypermutation. *Nature Reviews
466 Immunology*, 6(8):573–583, 2006.

467 [28] Aviv Omer, Ayelet Peres, Oscar L Rodriguez, Corey T Watson, William Lees, Pazit Polak,
468 Andrew M Collins, and Gur Yaari. T cell receptor beta germline variability is revealed by
469 inference from repertoire data. *Genome medicine*, 14:1–19, 2022.

470 [29] Aviv Omer, Or Shemesh, Ayelet Peres, Pazit Polak, Adrian J Shepherd, Corey T Watson,
471 Scott D Boyd, Andrew M Collins, William Lees, and Gur Yaari. Vdjbase: an adaptive
472 immune receptor genotype and haplotype database. *Nucleic acids research*, 48(D1):D1051–
473 D1056, 2020.

474 [30] Matt Pennell, Oscar L Rodriguez, Corey T Watson, and Victor Greiff. The evolutionary and
475 functional significance of germline immunoglobulin gene variation. *Trends in immunology*,
476 44(1):7–21, 2023.

477 [31] Ayelet Peres, Moriah Gidoni, Pazit Polak, and Gur Yaari. Rabhit: R antibody haplotype
478 inference tool. *Bioinformatics*, 35(22):4840–4842, 2019.

479 [32] Ayelet Peres, William D Lees, Oscar L Rodriguez, Noah Y Lee, Pazit Polak, Ronen Hope,
480 Meirav Kedmi, Andrew M Collins, Mats Ohlin, Steven H Kleinstein, Corey T Watson, and Gur
481 Yaari. IGHV allele similarity clustering improves genotype inference from adaptive immune
482 receptor repertoire sequencing data. *Nucleic Acids Research*, page gkad603, 08 2023.

483 [33] Christelle Pommie, Séverine Levadoux, Robert Sabatier, Gérard Lefranc, and Marie-Paule
484 Lefranc. IMGT standardized criteria for statistical analysis of immunoglobulin V-REGION
485 amino acid properties. *J. Mol. Recognit.*, 17(1):17–32, January 2004.

486 [34] Pradeepa Pushparaj, Andrea Nicoletto, Daniel J Sheward, Hrishikesh Das, Xaqin Castro
487 Dopico, Laura Perez Vidakovics, Leo Hanke, Mark Chernyshev, Sanjana Narang, Sungyong
488 Kim, et al. Immunoglobulin germline gene polymorphisms influence the function of sars-cov-2
489 neutralizing antibodies. *Immunity*, 56(1):193–206, 2023.

490 [35] Duncan K. Ralph and Frederick A. Matsen. Consistency of vdj rearrangement and substitu-
491 tion parameters enables accurate b cell receptor sequence annotation. *PLOS Computational
492 Biology*, 12(1):e1004409, January 2016.

493 [36] Oscar L Rodriguez, Yana Safanova, Catherine A Silver, Kaitlyn Shields, William S Gibson,
494 Justin T Kos, David Tieri, Hanzhong Ke, Katherine JL Jackson, Scott D Boyd, et al. Genetic
495 variation in the immunoglobulin heavy chain locus shapes the human antibody repertoire.
496 *Nature communications*, 14(1):4419, 2023.

497 [37] Modi Safran, Lael Werner, Ayelet Peres, Pazit Polak, Naomi Salomon, Michael Schvimer,
498 Batia Weiss, Iris Barshack, Dror S Shouval, and Gur Yaari. A somatic hypermutation–based
499 machine learning model stratifies individuals with crohn’s disease and controls. *Genome
500 Research*, 33(1):71–79, 2023.

501 [38] Geir Kjetil Sandve and Victor Greiff. Access to ground truth at unconstrained size makes
502 simulated data as indispensable as experimental data for bioinformatics methods development
503 and benchmarking. *Bioinformatics*, 38(21):4994–4996, 2022.

504 [39] David G Schatz and Yanhong Ji. Recombination centres and the orchestration of v (d) j
505 recombination. *Nature reviews immunology*, 11(4):251–263, 2011.

506 [40] Erand Smakaj, Lmar Babrak, Mats Ohlin, Mikhail Shugay, Bryan Briney, Deniz Tosoni,
507 Christopher Galli, Vendi Grobelsk, Igor D’Angelo, Branden Olson, Sai Reddy, Victor Greiff,
508 Johannes Trück, Susanna Marquez, William Lees, and Enkelejda Miho. Benchmarking im-
509 munoinformatic tools for the analysis of antibody repertoire sequences. *Bioinformatics*,
510 36(6):1731–1739, December 2019.

511 [41] Omri Snir, Luka Mesin, Moriah Gidoni, Knut EA Lundin, Gur Yaari, and Ludvig M Sollid.
512 Analysis of celiac disease autoreactive gut plasma cells and their corresponding memory com-
513 partment in peripheral blood using high-throughput sequencing. *The Journal of Immunology*,
514 194(12):5703–5712, 2015.

515 [42] Joel NH Stern, Gur Yaari, Jason A Vander Heiden, George Church, William F Donahue,
516 Rogier Q Hintzen, Anita J Huttner, Jon D Laman, Rashed M Nagra, Alyssa Nylander, et al.
517 B cells populating the multiple sclerosis brain mature in the draining cervical lymph nodes.
518 *Science translational medicine*, 6(248):248ra107–248ra107, 2014.

519 [43] Jason Anthony Vander Heiden, Susanna Marquez, Nishanth Marthandan, Syed Ahmad Chan
520 Bukhari, Christian E Busse, Brian Corrie, Uri Hershberg, Steven H Kleinstein, Frederick A
521 Matsen IV, Duncan K Ralph, et al. Airr community standardized representations for anno-
522 tated immune repertoires. *Frontiers in immunology*, 9:2206, 2018.

523 [44] Gur Yaari and Steven H Kleinstein. Practical guidelines for b-cell receptor repertoire sequenc-
524 ing analysis. *Genome medicine*, 7:1–14, 2015.

525 [45] Gur Yaari, Mohamed Uduman, and Steven H Kleinstein. Quantifying selection in high-
526 throughput immunoglobulin sequencing data sets. *Nucleic acids research*, 40(17):e134–e134,
527 2012.

528 [46] Gur Yaari, Jason A. Vander Heiden, Mohamed Uduman, Daniel Gadala-Maria, Namita
529 Gupta, Joel N. H. Stern, Kevin C. O'Connor, David A. Hafler, Uri Laserson, Francois Vi-
530 gneault, and Steven H. Kleinstein. Models of somatic hypermutation targeting and substi-
531 tution based on synonymous mutations from high-throughput immunoglobulin sequencing data.
532 *Frontiers in Immunology*, 4, 2013.

533 [47] Christina Yacoob, Marie Pancera, Vladimir Vigdorovich, Brian G Oliver, Jolene A Glenn,
534 Junli Feng, D Noah Sather, Andrew T McGuire, and Leonidas Stamatatos. Differences in
535 allelic frequency and cdrh3 region limit the engagement of hiv env immunogens by putative
536 vrc01 neutralizing antibody precursors. *Cell reports*, 17(6):1560–1570, 2016.

537 [48] Jian Ye, Ning Ma, Thomas L. Madden, and James M. Ostell. Igblast: an immunoglobulin
538 variable domain sequence analysis tool. *Nucleic Acids Research*, 41(W1):W34–W40, May
539 2013.

540 [49] Yan Zhu, Haipei Tang, Wenxi Xie, Sen Chen, Huikun Zeng, Chunhong Lan, Junjie Guan,
541 Cuiyu Ma, Xiujia Yang, Qilong Wang, et al. The multilevel extensive diversity across the
542 cynomolgus macaque captured by ultra-deep adaptive immune receptor repertoire sequencing.
543 *Science Advances*, 10(4):eadj5640, 2024.